electronics

MDPI

Article

Piecewise Hybrid System with Cross-Correlation Spectral Kurtosis for Fault Diagnosis in Rolling Bearing of Wind Power Generator

Shan Wang [1,2,*], Zijian Qiao [3] and Pingjuan Niu [4]

[1] Tianjin Key Laboratory for Advanced Mechatronic System Design and Intelligent Control, School of Mechanical Engineering, Tianjin University of Technology, Tianjin 300384, China
[2] National Demonstration Center for Experimental Mechanical and Electrical Engineering Education, Tianjin University of Technology, Tianjin 300384, China
[3] School of Mechanical Engineering and Mechanics, Ningbo University, Ningbo 315211, China; qiaozijian@nbu.edu.cn
[4] School of Electronics and Information Engineering, Tiangong University, Tianjin 300384, China; niupingjuan@tiangong.edu.cn
* Correspondence: wangshan@email.tjut.edu.cn

Abstract: As the core equipment of wind turbines, rolling bearings affect the normal operation of wind power generators, resulting in huge economic losses and significant social impacts in the case of faults. Most faults are not easily found because of the small vibration response of these rolling bearings that operate in harsh conditions. To address the problem that the fault identifications of rolling bearings are disturbed by the strong noise in wind power generators, an adaptive nonlinear method based on a piecewise hybrid stochastic resonance system with a novel cross-correlation spectral kurtosis is proposed. Then, the vibration signals collected from the fault point of the outer and inner rings are used to clarify the outstanding capability of the proposed method when compared with the maximum cross-correlation-kurtosis-based unsaturated stochastic resonance method. Furthermore, the machine learning method based on the medium tree was adopted to further prove the excellent performance of the piecewise hybrid stochastic resonance system with a novel cross-correlation spectral kurtosis for realizing the efficient detection of rolling bearing faults in wind power generators, which has important innovation significance and practical engineering value for ensuring the safe and stable operation of wind turbines.

Keywords: piecewise hybrid stochastic resonance; cross-correlation spectral kurtosis; fault diagnosis; wind power generator; rolling bearing; stochastic resonance

Citation: Wang, S.; Qiao, Z.; Niu, P. Piecewise Hybrid System with Cross-Correlation Spectral Kurtosis for Fault Diagnosis in Rolling Bearing of Wind Power Generator. *Electronics* **2023**, *12*, 1548. https://doi.org/10.3390/electronics12071548

Academic Editors: Katarzyna Antosz, Jose Machado, Yi Ren, Rochdi El Abdi, Dariusz Mazurkiewicz, Marina Ranga, Pierluigi Rea, Vijaya Kumar Manupati, Emilia Villani and Erika Ottaviano

Received: 13 February 2023
Revised: 18 March 2023
Accepted: 23 March 2023
Published: 25 March 2023

1. Introduction

Energy is a necessary condition for economic development and plays an irreplaceable role in promoting human historical progress. Fossil fuels, such as natural gas, oil, and coal, have important positions in the energy supply [1,2]. Wind energy is a renewable energy and is meaningful for large energy storage with the flash point of being sustainable and pollution-free. Compared with hydropower and nuclear energy, the development of wind energy has little impact on the natural and ecological environments, low danger risk, and no secondary pollution to the environment. Meanwhile, compared with solar energy, the utilization of wind energy is unrestricted by objective factors such as the season, climate, and region [3,4]. Therefore, wind energy is considered to be the most promising renewable source in the future.

The high cost of the rapid development of wind power generators includes the operation and maintenance [5,6]. The operational quality of wind power generators is tested in harsh working environments including extreme weather conditions such as lightning, rainstorms, ice and snow, wind and sand in desert areas, and salt fog at sea [7,8]. The results

show that the impact load on each component changes in real time, and an uncontrollable impact significantly increases the probability of a fault under the action of an alternating load. Wind turbines can convert mechanical energy into electrical energy, which is an important component. The energy conversion of wind turbines depends on the rotation of bearings [9,10]. Furthermore, the fault rate of wind turbine bearings is significantly higher than that of bearings under normal operation. If the inherent bearings encounter faults, the wind turbine is difficult to operate in an extreme environment. Moreover, it is inconvenient to hoist and replace mechanical transmission components, and the maintenance is extremely difficult and expensive [11]. Accordingly, the fault diagnosis of the running state of rolling bearings has important practical significance for the stable operation of wind turbines and reducing economic losses [12].

However, the fault features of wind turbine bearings are always too weak to detect for complex noise [13,14]. The key to extracting the bearing fault signals is to extract a weak signature under a strong background noise. Many researchers have used novel methods and technologies to explore wind turbine bearing fault extraction. Herp et al. [15] studied the Gaussian process and Bayesian reasoning methods, and applied them to wind turbine state prediction, which can achieve a high accuracy prediction of bearing faults. Shi et al. [16] proposed the innovative empirical mode decomposition method and applied it to the cascaded multi-stable stochastic resonance system, which not only reduced the decomposition layers, but also efficiently removed the high-frequency noise. Combined with bidirectional long short-term memory, Xu et al. [17] developed a multiscale convolutional neural network model to improve the generalization ability in complex working and testing environments to extract the fault feature by the intelligent models. However, accurate diagnostic results of characteristic frequencies are difficult to obtain using traditional methods for vibration signal analysis, therefore, requiring more advanced methods. Wang et al. [18] proposed an unsaturated stochastic resonance (USR) theory with the detection index of the maximum cross-correlation kurtosis (MCCK), which improved the fault diagnosis ability of rolling bearings. Lu et al. [19] analyzed a full-wave signal construction algorithm to improve the capability of stochastic resonance to extract the fault feature. Li et al. [20] proposed a new stochastic resonance method under frequency shift multi-scale noise, and the target signal moved into the designated low-frequency domain via the newly proposed method, which was applied to improve the bearing fault features from the wind turbine. The above methods are of great significance in research on the weak bearing fault diagnosis. Furthermore, the stochastic resonance method was employed to extract the fault features of rolling bearings. However, when detecting the fault signatures of wind turbine bearings in a background of strong noise, the accuracy of system detection using the stochastic resonance method still requires improvement.

In recent years, researchers have conducted in-depth studies on the evaluation models of rolling bearing inspection systems. By constructing a composite function of the feedback strength, delay time, and signal-to-noise ratio, Xia et al. [21] combined the delay time with the best feedback strength, reconstructed the delay feedback stochastic resonance, effectively improved the signal-to-noise ratio, and accurately extracted the fault signature frequency. Li et al. [22] studied the tri-stable potential function and its shape change characteristics; introduced delay, feedback, and damping parameters; and considered the output signal-to-noise ratio (SNR) as the evaluation standard, which determined the parameter optimization effect of the adaptive algorithm and improved the ability to extract weak fault information. Antoni [23] investigated a method for bearing fault diagnosis with spectra, which was defined as the evaluation function, selected the frequency band sensitive to pulse characteristics, extracted the vibration signals in this frequency band, and identified the bearing fault diagnosis. Elforjani et al. [24] proposed a signal strength estimation method, which was superior to the traditional wave crest factor and kurtosis index and was suitable for fault detection of mechanical components in terms of the early fault detection of fan bearings. Jing et al. [25] studied the generalized correlation coefficient and adaptive stochastic resonance, which can be combined to process the vibration signal. Tao et al. [26]

studied the measurement index and proposed the cross-correlation coefficient for the feature extraction of the stochastic resonance method when processing multi-frequency periodic signals. However, the traditional detection index affected the extraction ability of the rolling bearing fault feature frequency.

In this study, a nonlinear system based on the adaptive piecewise hybrid stochastic resonance (APHSR) model was proposed, and an innovative cross-correlation spectrum kurtosis (CSK) is defined as the detection index of the APHSR model to automatically derive the characteristic frequency of rolling bearings. Cooperating with Beijing Vrita Measurement and Control System Co., Ltd.,Beijing, China, vibration data were collected regarding the rolling bearing faults located on the outer and inner rings in wind turbines. Compared with the USR method with the MCCK index, the proposed method had a higher performance on fault frequency detection. Furthermore, 300 groups of original signals and signals were processed by the CSK-based APHSR method and CSKMCCK-based USR method, and then machine learning was employed to determine the recognition rate. Furthermore, the advantages of the CSK-based APHSR method are verified to improve the current weak bearing fault diagnosis ability in wind power generator under a strong noise background. Furthermore, we designed the fault diagnosis software of the rolling bearing of the wind turbine using the method proposed in this manuscript, and, cooperating with Beijing Veritas Measurement and Control System Co., Ltd., Beijing, China, combining the developed online monitoring vibration data acquisition and control software of the wind turbine and the online monitoring data acquisition software of the wind turbine, the real-time bearing vibration signal was collected and inputted into the bearing fault diagnosis software to determine the bearing status, which can be realized for the online detection of errors caused by the vibration of wind turbine bearings and preventing faults with the CSK-based APHSR method.

The structure of the manuscript is organized below. The CSK-based APHSR method is briefly introduced in Section 2, which goes deeply into the benefits of noise and enhances the weak signature through an adaptive piecewise hybrid stochastic resonance method with the detection index of the CSK function. Subsequently, vibration signals, including the fault points of rolling bearings located on the inner and outer rings of the wind power generator, were processed by the CSK-based APHSR method and the USR method with the MCCK index, as presented in Section 3. In addition, an artificial intelligence-based technique was employed to verify the recognition rate of 300 groups of signals generated from the original signals and processed using the CSK-based APHSR method, as well as the USR method with the MCCK index. Finally, Section 4 summarizes the conclusions of this manuscript.

2. Formulation Analysis

2.1. Adaptive Piecewise Hybrid Stochastic Resonance Model

Generally, a nonlinear system is constructed using piecewise hybrid stochastic resonance, and the corresponding Langevin equation is [27] expressed as follows:

$$\mathrm{U}(x) = \begin{cases} -\frac{\sqrt{\mathrm{a}^3/b}}{4(\mu-1)}(x+\mu\sqrt{a/b}), x < -\sqrt{a/b}, \\ -\frac{\mathrm{a}}{2}x^2 + \frac{b}{4}x^4, \ \sqrt{a/b} \le x \le -\sqrt{a/b}, \\ \frac{\sqrt{\mathrm{a}^3/b}}{4(\mu-1)}(x-\mu\sqrt{a/b}), x > \sqrt{a/b}. \end{cases} \quad (1)$$

where a and b are all of the positive parameters, and μ is a parameter which cannot be equal to one. $s(t)$ is the periodic signal and $n(t)$ is the noise signal, which is equal to zero. The potential function $V(x)$ of the piecewise hybrid stochastic resonance is expressed as follows:

$$V(x) = U(x) - xA\cos(2\pi f_0 t + \phi). \quad (2)$$

In addition, a critical amplitude was set to ensure that the stochastic resonance system maintains a bistable structure. When $A\cos(2\pi f_0 t + \phi)$ reaches the extreme value, it will be a multi-stable structure for the potential function instead of being bistable. Consequently, the smaller the critical amplitude is, the easier it is to achieve a stochastic resonance station. $A\cos(2\pi f_0 t)$ achieves the maximum when $t = -\phi/(2\pi f_0)$, and the expression of $U(x)$ of traditional stochastic resonance is functioned as [28]:

$$\begin{cases} \frac{dU(x)}{dx} = -ax + bx^3 - A = 0, \\ \frac{d^2U(x)}{dx^2} = -a + 3bx^2 = 0 \end{cases} \tag{3}$$

Accordingly, the critical amplitude of the APHSR method is shown below:

$$\begin{cases} \frac{dU(x)}{dx} = -\frac{\sqrt{a^3/b}}{4(\mu-1)} - A = 0, x < -\sqrt{a/b}, \\ \frac{dU(x)}{dx} = -ax + bx^3 - A = 0, -\sqrt{a/b} \le x \le \sqrt{a/b}, \\ \frac{dU(x)}{dx} = \frac{\sqrt{a^3/b}}{4(\mu-1)} - A = 0, x > \sqrt{a/b}. \end{cases} \tag{4}$$

The critical amplitude is obtained as follows:

$$Ac = \begin{cases} -\frac{\sqrt{a^3/b}}{4(\mu-1)}, x < -\sqrt{a/b}, \\ \sqrt{\frac{4a^3}{27b}}, -\sqrt{a/b} \le x \le \sqrt{a/b}, \\ \frac{\sqrt{a^3/b}}{4(\mu-1)}, x > \sqrt{a/b}. \end{cases} \tag{5}$$

We set the input signal as $s(t) = A\cos(2\pi f t)$, the three parameters of the stochastic resonance method were $a = b = 0.5$, f was the frequency with the value of 0.01 Hz, f_s was the sampling frequency with the value of 10 Hz, the amplitude was $A = 0.5$ V [29], and the parameter μ was varied as $\mu = \sqrt{1.5}, \sqrt{1.75}, \sqrt{2}, \sqrt{3}, 2$. Figure 1a shows that the A_c of the theory decreased with the increase of the parameter μ, and was even lower when compared with the USR method when $\mu = \sqrt{2}$ and the classical bistable stochastic resonance (CBSR) model when $\mu = 3\sqrt{3}/8$. Figure 1b shows the results of the numerical simulation of the APHSR method, where the output amplitude increased with the increasing μ, which indicated its great significance.

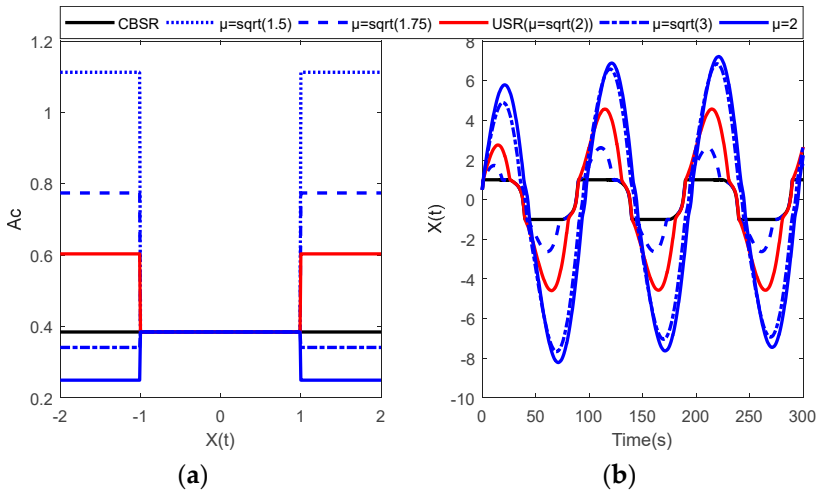

Figure 1. Critical amplitudes and outputs via three different methods with parameter μ.

To further verify parameter μ, the adiabatic approximation theory and Kramer's escape rate were used to obtain the formula derivation of Kramer's escape rate. According

to the adiabatic approximate theory [30,31], the formula of Kramer's time is expressed as follows:

$$r_{-}^{-1}(t) = \frac{1}{D}\left[\int_{-\mu\sqrt{a/b}}^{-\sqrt{a/b}} \exp\left[-\frac{\sqrt{a^3/b}}{4D}\left(\frac{x+\mu\sqrt{a/b}}{1-\mu}\right)\right]dx\right] \times \left[\int_{-\sqrt{a/b}}^{0} \exp\left[\frac{1}{D}\left(-\frac{a}{2}x^2+\frac{b}{4}x^4\right)\right]dx\right]. \quad (6)$$

where $\tau_{\pm}$ is the mean first passage time. Under the conditions of D << 1,A << 1 [32], it can be obtained for the final results that:

$$r_{-}^{-1}(t) \approx \frac{4(\mu-1)}{a}\exp\left(\frac{a^2}{4bD}\right). \quad (7)$$

Accordingly,

$$\begin{aligned} r_{+}^{-1}(t) &= \frac{1}{D}\left[\int_{0}^{\sqrt{a/b}} \exp\left[\frac{1}{D}\left(-\frac{a}{2}x^2+\frac{b}{4}x^4\right)\right]dx\right] \times \left[\int_{\sqrt{a/b}}^{\mu\sqrt{a/b}} \exp\left[\frac{\sqrt{a^3/b}}{4D}\left(\frac{x+\mu\sqrt{a/b}}{1-\mu}\right)\right]dx\right] \\ &\approx \frac{4(\mu-1)}{a}\exp\left(\frac{a^2}{4bD}\right). \end{aligned} \quad (8)$$

Therefore, the formula of Kramer's escape rate of the piecewise hybrid stochastic resonance theory is:

$$r_k = \frac{a}{4(\mu-1)}\exp\left(-\frac{a^2}{4bD}\right). \quad (9)$$

The input signal of the bistable theory was set as $s(t) = A\cos(2\pi ft)$, the theory parameters a and b were set to 1, signal frequency f was set to 0.15 Hz, the sampling frequency f_s was set to 10 Hz, the amplitude A was set to 1.2 V, and the new μ values were $\mu = \sqrt{1.5}, \sqrt{1.75}, \sqrt{2.0}, \sqrt{3.0}, 2.0$. From Figure 2, it can be seen that Kramer's escape rate of the APHSR theory was always higher than that of the CBSR method and higher than that of the USR theory when $\mu > \sqrt{2}$. It is clear that μ had an effective influence on the escape rate and the stochastic resonance generation.

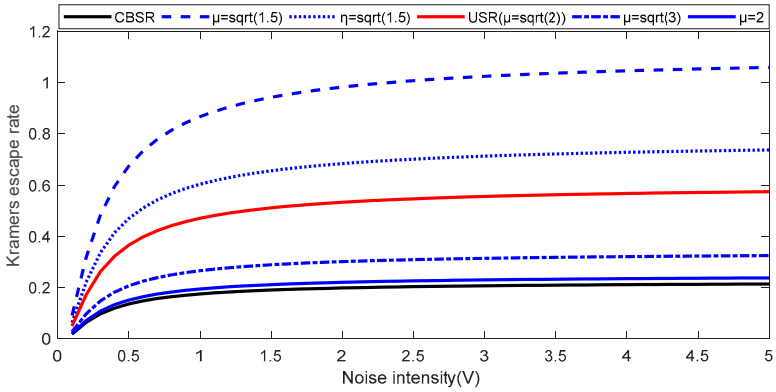

Figure 2. Kramer's escape rate results via three different methods with parameter μ.

The APHSR theory exhibited a higher amplitude and clearer output compared with the CBSR and USR theories. Moreover, the results indicated that the APHSR theory was more robust for detecting weak signals under heavy noise.

2.2. Novel Evaluation Function of Cross-Correlated Spectrum Kurtosis

The kurtosis (K) index is a dimensionless parameter, and is particularly sensitive to impact signals, which is especially suitable for the diagnosis of surface damage faults. The

kurtosis value of the vibration signal, X_o, via a stochastic resonance system should be satisfied as [33,34]:

$$K(\widetilde{X}) = \frac{E(\left|\widetilde{X_o}\right|^4)}{\left[E(\left|\widetilde{X_o}\right|^2)\right]^{2'}}. \tag{10}$$

where the mathematical expectation operator is expressed as $E(\cdot)$.

Furthermore, the correlation coefficient (C) indicates the closeness of the correlations between two random variables. When the closeness is higher than a certain value, then the two random variables are related. Otherwise, it is irrelevant. Function C was calculated between signals using [35]:

$$C = \frac{\sum_{n=1}^{2N-1} X_o(n)X_i(n)}{\sqrt{\sum_{n=1}^{2N-1} X_o^2(n) \sum_{n=1}^{2N-1} X_i^2(n)}}. \tag{11}$$

where N represents the sampling points of signal.

As shown, the kurtosis value is usually considered to express the signatures of the signal around its average value, and has the advantages in characterizing the transient pulse, while C can be used to measure the relevant information between vibration signals. Therefore, the cross-correlation spectral kurtosis index function is designed based on the advantages of the kurtosis function and the cross-correlation function to quantitatively evaluate the detection ability of the bearing fault system under the background of complex noise in the frequency domain, as is expressed below:

$$\mathrm{CSK} = \frac{\mathrm{n}\sum_{n=1}^{N}\left[\left|R_s(n) - \overline{R_s}\right|^2 \cdot \left|Y_s(n) - \overline{Y_s}\right|^2\right]}{\sum_{n=1}^{N}\left|R_s(n) - \overline{R_s}\right|^2 \cdot \sum_{n=1}^{N}\left|Y_s(n) - \overline{Y_s}\right|^2}. \tag{12}$$

where Y_s represents the spectrum of the output signal X_o, $\overline{Y}_s$ represents the mean of Y_s, R_s represents the spectrum of the pulse signals $R_n(t)$, which is used to generate a series of transient fault features. $\overline{R}_s$ is the mean of R_s,and $R_n(t)$ can be expressed as the following simulation model [36,37]:

$$R_n(t) = B(t)\sum_q R(t - q/f_0) + N(t). \tag{13}$$

where q represents the number of transients, $B(t)$ denotes the repetitive transients' amplitude, $N(t)$ represents random noise, and f_0 denotes the frequency of fault feature. The function of periodic impulse is $R(t)$, which is given by:

$$R(t) = \begin{cases} \exp(-\beta_w t)\sin(2\pi f_{re} t), t > 0, \\ 0, \qquad\qquad\qquad t \le 0. \end{cases} \tag{14}$$

where f_{re} represents the resonance frequency, β_w represents the structural damping ratio, the sampling frequency is f_s, and the sampling time is t.

2.3. Proposed CSK-Base APHSR system

For the proposed model, CSK was the evaluation criterion for the parameters determined by the three-dimensional reverse positioning methods. Figure 3 depicts the corresponding flowchart.

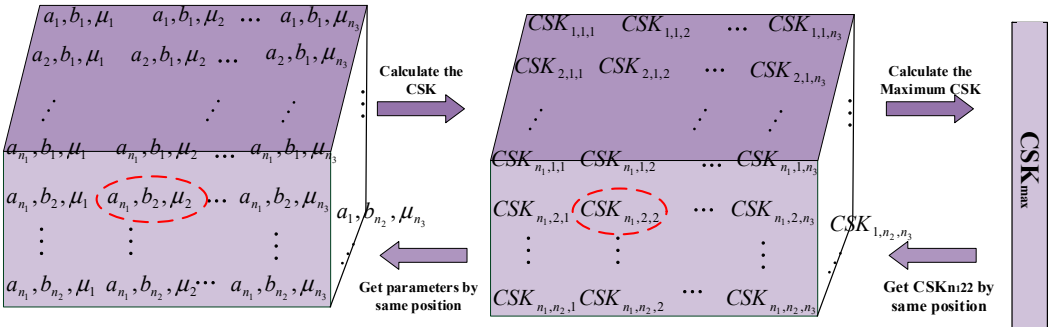

Figure 3. Flowchart of adaptive APHSR theory.

It can be seen from Figure 3 that n_1, n_2, and n_3 were the cycles of parameters a, b, and μ of the APHSR theory, respectively. The form of CSK was a matrix (n_1, n_2, n_3). We set and changed the parameters a, b, and μ step-by-step and calculated and stored the CSK values of the output signal in the matrix. Then, we calculated the maximum value of the CSK matrix. According to the position of CSKmax, the three-dimensional reverse positioning method was applied to automatically locate the position of the optimal parameters a, b, and μ [38].

As shown in Figure 4, the APHSR method was adopted with a new detection function CSK aimed at the research problem of rolling bearing faults located on the wind power generator, which can intelligently analyze the obtained signals, as well as identify the characteristic frequency of rolling bearing faults. The diagrammatic sketch using the CSK-based APHSR method for weak fault detection from a wind power generator bearing is shown as below:

1. Pre-processing of signals: the empirical mode decomposition method was used for the vibration signals obtained from wind power generators to obtain intrinsic mode functions. The energy density and the correlation coefficient methods were used to reduce high- and low-frequency noises, respectively [39]. Therefore, a filtered signal could be acquired when the remaining components were reconstructed.
2. Determination of the optimal parameters: the scopes of parameters a, b, and μ were set as (0, 20], (0, 20], and (0, 1)∪(1, 3), respectively, and CSK was calculated as the parameters varied. Thereafter, the three-dimensional reverse positioning method was used for obtaining the optimal parameters of the APHSR method from the corresponding position.
3. Extraction of fault feature: with the optimal condition of the APHSR theory, the fault characteristics of vibration signals under heavy background noise were effectively detected. Furthermore, machine learning based on a medium tree was adopted to verify the outstanding ability of the CSK-based APHSR method on intelligent feature frequency detection.

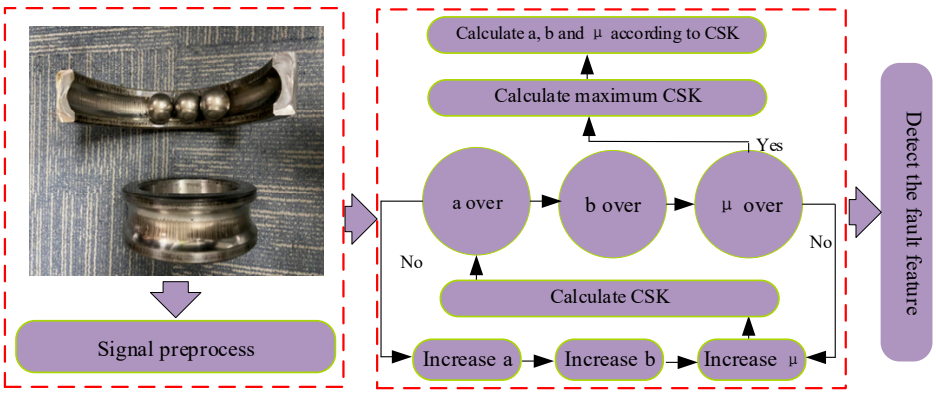

Figure 4. Proposed CSK-based APHSR method for bearing fault feature of wind power generator.

3. Engineering Applications

As an important mechanism equipment to obtain electrical energy converting from green wind energy, the basic structure of wind turbines comprises blades, a transmission system, and a generator. Wind power generators are one of the most critical components of wind turbine equipment. Once the fault occurs, it causes major economic losses because bearings are widely used in wind power generation. To reduce the risk of the catastrophic fault of the machine and to ensure the safety of personnel, it is meaningful to study the weak fault extraction of rolling bearings located on the wind turbine.

The maintenance personnel found abnormal noises in the wind turbine at the XX wind power generation work site. When there is a damage on the local surface of the gearing, bearings, or shafts of wind power generators and the element passes through a certain defect, a weak impact signal is generated. The impact energy generated in the gearing, bearings, or shafts can excite the vibration of the natural frequency of each component, and the vibration energy will decrease with the damping of the mechanical structure. The impact pulse signal generated by the local defects has different specific frequencies at different positions, and its size is determined by the rotation speed and model. Therefore, the fault location on gearing, bearings, or shafts is located according to different feature frequencies. With cooperation from Beijing Vrita Measurement and Control System Co., Ltd., Beijing, China, as is shown in Figure 5, a diagnosis system of CSK-based APHSR method for fault bearings located on wind power generator is designed for improving the detection performance and conducting a detailed inspection of the rolling bearings in a wind turbine.

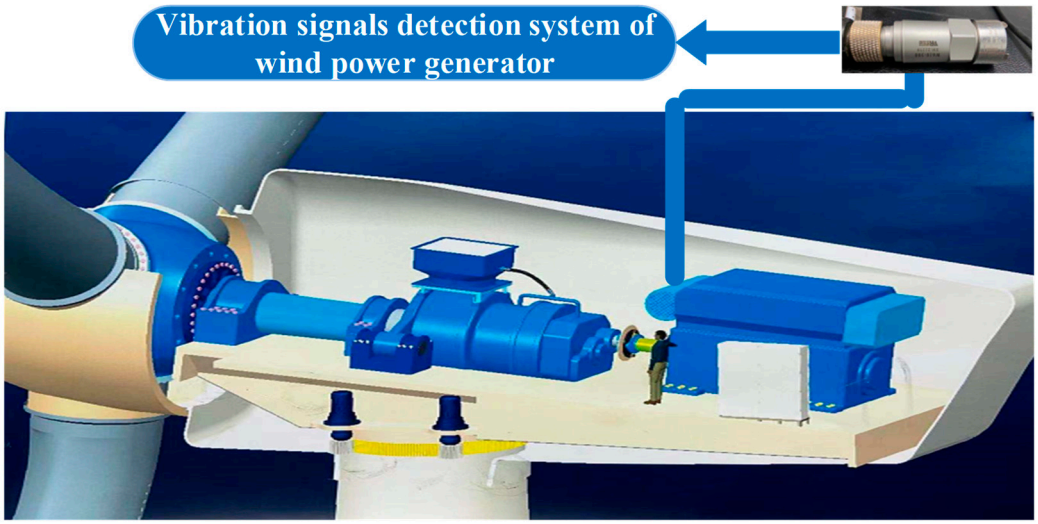

Figure 5. Vibration signals detection system of rolling bearing embedded in wind turbine generator.

3.1. Outer Ring Fault of Bearing

The maintenance personnel detected the internal structure of the drive end of the XX wind power generator, and a schematic of its constituent rolling bearing is presented in Figure 6. Dents with faults can be observed on the rolling bearing's outer ring at the driving end of the wind power generator.

Under the action of the wind, the wind turbine blades are driven to rotate, and the speed is raised and transmitted to the generator through the speed increase gearbox, which is the working principle of the wind turbine generator. The stable speed of the wind turbine was 1700–1800 r/min. The test point was located at the radial position at the driving end of the wind power generator. Data acquisition was started using the control software, and the vibration signal of the test point was collected through the acceleration sensor. As an important element, the sensor used in the fault diagnosis system of the wind power generator of rolling bearing was a piezoelectric acceleration sensor, which uses piezoelectric material as the conversion element and its output is an electrical signal

proportional to the acceleration. Through the acceleration sensor, the bearing vibration signal was converted into electrical signal. The WindCMS data collector, developed by Beijing Veritas Measurement and Control System Co., Ltd., Beijing, China, collected the vibration data of the rolling bearing and then inputted it to the proposed CSK-based APHSR method for processing. We set the number of sampling points as 65,536, the rotating speed as 1805.37 rpm, and the sampling frequency f_s as 25.6 kHz. The parameters of the rolling bearings of the wind power generator are listed in Table 1.

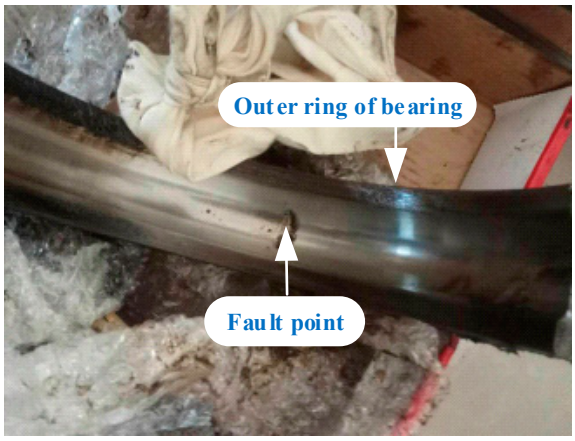

Figure 6. Outer ring fault of rolling bearing at driving end of wind power generator.

Table 1. Bearing parameters.

Component	Mfg.	Bearing No.	# of R. E.	Outer Ring (Multiple of Running Speed in Hz)	Inner Ring (Multiple of Running Speed in Hz)
Bearing	NSK	6328	8	3.134 f_r	4.866 f_r

According to the vibration analysis theory and the fault rolling bearing parameters of the wind power generator detailed from Table 1, the rotation frequency of motor bearing was 30.09 Hz. After theoretical calculations, the values of fault feature frequency of the outer ring and inner ring were 94.3 Hz and 146.42 Hz, respectively. Figure 7 displayed the collected vibration data in the time and frequency domain.

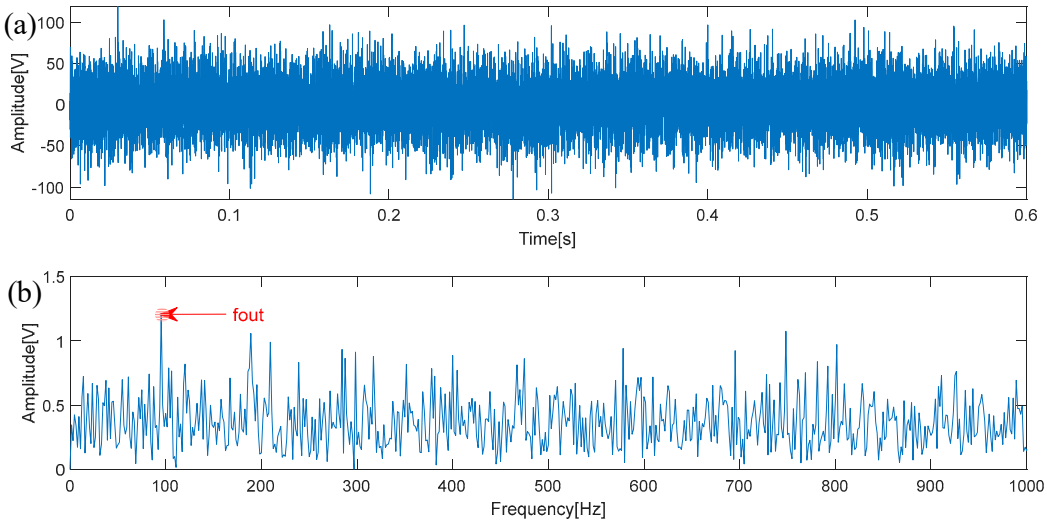

Figure 7. Waveform and spectra of outer ring bearing vibration signals of wind power generator.

As shown in Figure 7a, the bearing fault surrounded by the complex background noise in time domain was unclear. From Figure 7b of the frequency-domain spectra, the peaks of

the fault feature frequency at the bearing outer ring and its harmonics could not be seen obviously, where the fault feature frequency at the bearing outer ring and its harmonics were submerged by complex background noise. Thus, it is difficult to extract the bearing fault of the outer ring due to the high levels of noise at the feature frequency of 95.31 Hz.

The vibration signals were inputted into the APHSR method with the CSK index and USR method with the MCCK index. The parameters of $R_{\mathrm{n}}(\mathrm{t})$ were set as $\beta_w = 666.67$, $f_{re} = 1683.4$ Hz, $f_0 = 95.3$ Hz, and $t = 0.64$ s. After applying the CSK-based APHSR method, we performed the calculations using the optimal parameters of $a = 5$, $b = 1.2$, and $\mu = 2$. From Figure 8c,d, the waveform and spectrum of the processed signals are displayed, respectively. The peaks of the fault feature frequency at the bearing outer ring was eye-catching, with a value of 95.31 Hz, and was consistent with the theoretical value (94.3 Hz) and extracted the fault on the outer ring bearing. Meanwhile, the noise energy had been transferred and weakened via the APHSR method with the CSK index and the energy of the fault feature had been amplified. Furthermore, the SNR value of output signal was −11.1586 dB, and increased by 33.3288 dB when compared with the initial signals. The optimal parameters of the USR method with the MCCK index were calculated as $a = 10$ and $b = 0.7$. From Figure 8a,b, although the feature frequency can be observed by the MCCK-based USR method, a lot of noise was presented from the running environment, and the SNR value of output signal was −15.0771 dB and decreased by 3.9185 dB when compared with the CSK-based APHSR method. Therefore, the results indicated the excellent ability of the proposed method to extract noised vibration signals from a wind power generator.

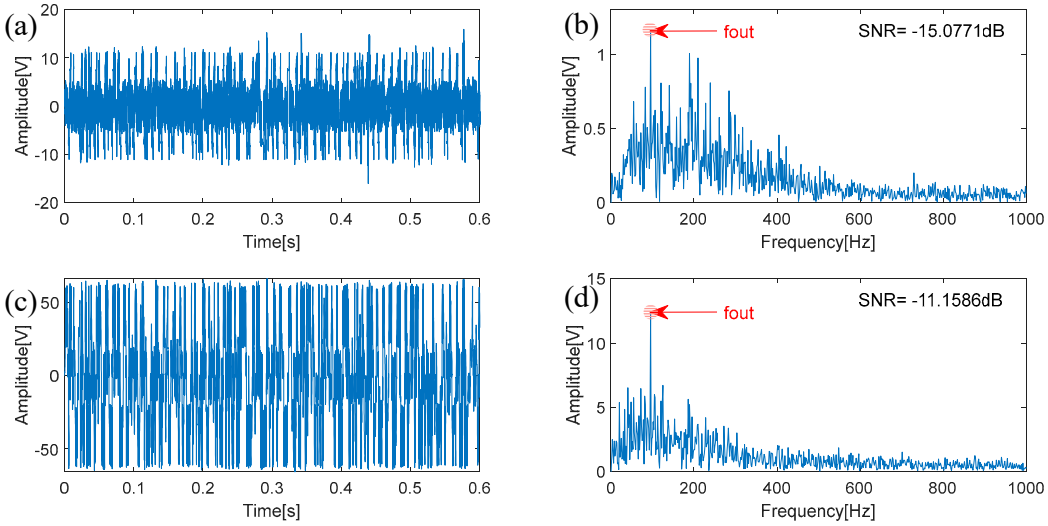

Figure 8. Waveform and spectra of outer ring signals processed by MCCK-based USR method and CSK-based APHSR method.

For further study of the diagnosis ability of the rolling bearing with the wind power generator, the machine learning method based on the medium tree was adopted on the engineering signals, including the original signals from the drive end of the wind power generator and those signals processed by MCCK-based USR and CSK-based APHSR methods. As is known, using artificial intelligent method to realize the bearing fault diagnosis requires numerous training samples. Therefore, the vibration signal was truncated by the segmented overlapping interception method. The intercept from the first point of the vibration signal to the n_{th} point was taken as the sample of the first signal, and the intercept from $(n - m)$ points to $(2n - m)$ points was taken as the sample of the second signal until the end of the signal. The total N samples were taken to complete the sample signal interception. Figure 9 shows the recognition rates of 300 groups of outer ring fault of the original signals and signals processed by two different methods.

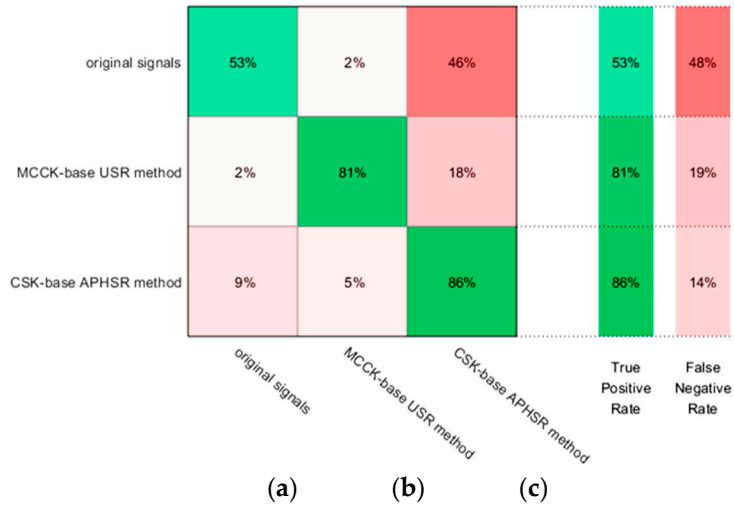

Figure 9. Recognition rates of outer ring: (**a**) original signals, and signals processed by (**b**) MCCK-based USR method and (**c**) CSK-based APHSR method.

Based on the confusion matrix, although 9% of data were misidentified as original signals and 5% of data were misidentified as the CSKMCCK-based USR method, the CSK-based APHSR method exhibited the highest recognition rate of approximately 86%, which was 33% and 5% greater when compared with the original signals and the CSKMCCK-based USR method. The result demonstrated the higher performance of the CSK-based APHSR method than the CSKMCCK-based USR method.

3.2. Inner Ring Fault of Bearing

The staff detected the internal structure of the driving end of a certain type of wind power generator. A diagram of the rolling bearing is provided in Figure 10. Many dents were apparent on the inner ring of the rolling bearing at the driving end of the wind power generator, which affected the healthy operation of the wind turbine and the economic benefits.

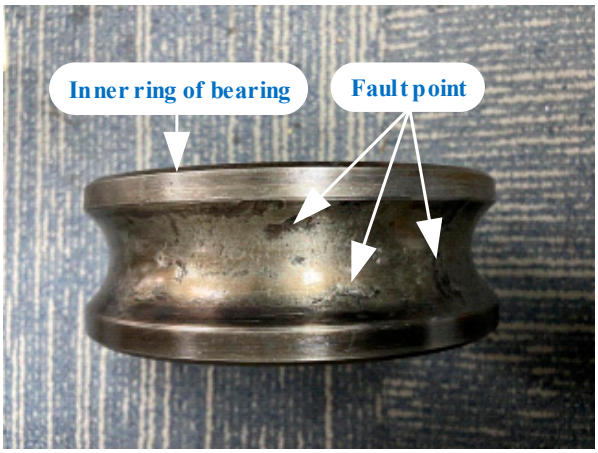

Figure 10. The inner ring fault of rolling bearing at driving end of wind power generator.

The test point was located at the radial position at the driving end of the wind turbine. Data acquisition started using the control software, and the vibration signal of the test point was collected through the acceleration sensor. The data from the driving end of the generator were extracted and analyzed using the proposed CSK-based APHSR method. We set the rotating speed as 1802.45 rpm, the number of sampling points as 65,536, and the sampling frequency f_s as 25.6 kHz. Table 1 presented the parameters of the generator rolling bearings.

Based on the vibration analysis theory, the bearing rotation frequency of the wind power generator was calculated as 30.04 Hz, and the theoretically evaluated fault frequency of the bearing inner rings was calculated as 146.17 Hz. To acquire the feature frequency, the waveform and spectra of the input signals for the collected vibration signals of wind power generator are presented in Figure 11. Depending on the input bearing vibration signals, whether the fault existed at the inner ring could not be judged because the weak fault feature occurring on the inner ring were surrounded by the external complex noise and interference of the measuring instruments. We noted that determining the fault characteristic frequency of 146.5 Hz either from the waveform or the spectra was imprecise because of the complex noise. Moreover, it was worth noting that the rotation frequency amplitude was higher than the characteristic frequency of the fault located on the inner ring.

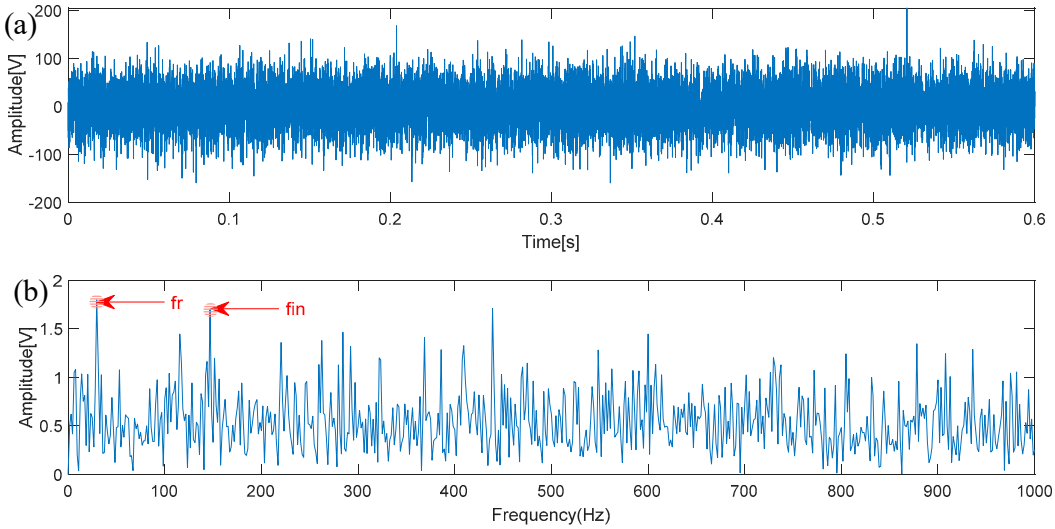

Figure 11. Waveform and spectra of inner ring bearing vibration signals of wind power generator.

To decrease the potential danger from the fault bearing of wind power generator and to improve the economic benefits of the wind turbines, the vibration signals were processed using the CSK-based APHSR method, as well as the MCCK-based USR method. The parameters of $R_{\mathrm{n}}(\mathrm{t})$ were set as $\beta_w = 666.67$, $f_{re} = 1683.4$ Hz, $f_0 = 146.5$ Hz, and $t = 0.64$ s. After applying the APHSR method with the CSK index, we performed the calculations for the optimal parameters set as $a = 0.47$, $b = 0.34$, and $\mu = 0.2$. From Figure 12c,d it can be seen that the energy of noise in the raw vibration signal had been transferred and eliminated, and the spectral peak at the inner ring fault feature was dominant, indicating the very clear feature frequency of 146.5 Hz consistent with the theoretical value of 146.17 Hz and demonstrating the extraction of the fault on the outer ring bearing. That is, the CSK-based APHSR method was capable of eliminating the noise energy and improving the fault feature energy submerged in the complex noise. Furthermore, the SNR value of the output signals was -14.5513 dB, and increased by 32.2912 dB when compared with the initial signals. Meanwhile, the amplitude of the rotation frequency was lower than the feature frequency of the inner ring fault. Regarding the USR method with the MCCK index, it was calculated for the optimal parameter values set as $a = 1.6$ and $b = 0.1$, and the corresponding waveform and spectra of the CSKMCCK-based USR method are presented in Figure 12a,b, respectively. A high rotation frequency could lead to incorrect judgment results, and the weak fault of the inner ring could be ignored. Furthermore, the SNR value of output signals of the proposed CSK-based APHSR method increased by 7.3528 dB compared with the CSKMCCK-based USR method. The results demonstrated the better performance of the CSK-based APHSR method on signal's detection from complex noise.

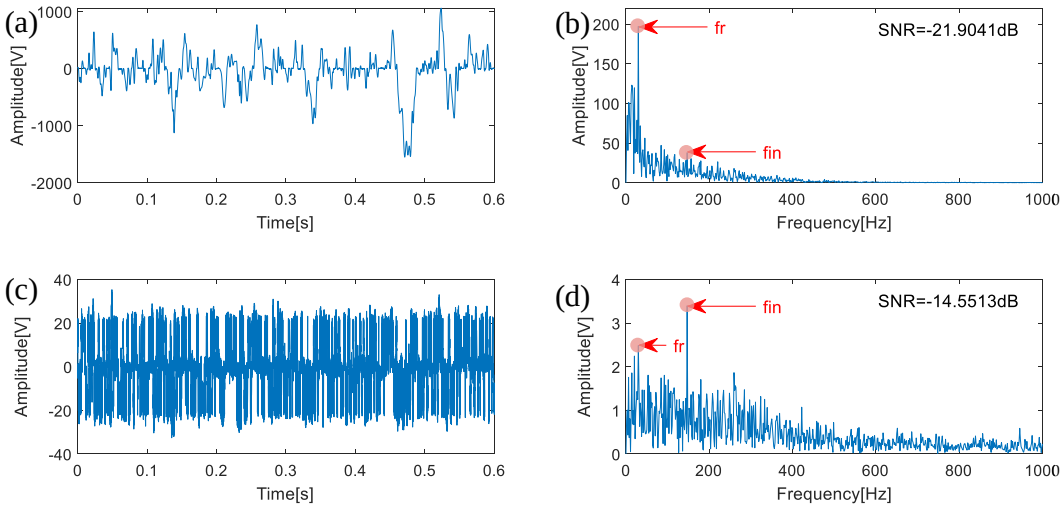

Figure 12. Waveform and spectra of inner ring signals processed by MCCK-based USR method and CSK-based APHSR method.

Similarly, machine learning based on the medium tree method was applied on the inner ring fault of motor bearing signals, including the original signals from the drive end of the wind power generator and those processed by the CSKMCCK-based USR and CSK-based APHSR methods. Figure 13 shows the recognition rates of 300 groups of inner ring fault of original signals and signals processed by two different methods.

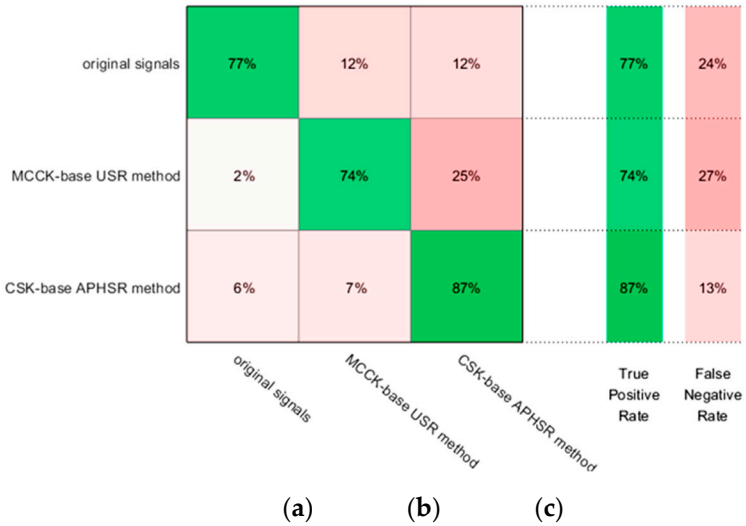

(**a**) (**b**) (**c**)

Figure 13. Recognition rates of inner ring: (**a**) original signals, and signals processed by (**b**) CSKMCCK-based USR method and (**c**) CSK-based APHSR method.

Based on the confusion matrix, the recognition rate of the original signals was 77% and decreased by 10% when compared with the CSK-based APHSR method. Meanwhile, the recognition rate of the CSKMCCK-based USR method was 74%, which was 3% lower than the original signals and 13% lower than the CSK-based APHSR method because the amplified characteristic frequency during signal processing was the rotation frequency.

The above engineering results demonstrated the outstanding performance of the CSK-based APHSR method to detect the bearing fault features embedded in background noise from the operating environment.

4. Conclusions

This study proposed an APHSR method with a novel measurement technique to optimize the adjusted parameters and enhance the performance of the fault frequency diagnosis of wind power generators with complex noise. The results of the identification on the bearing vibration signal of wind power generator are summarized as follows.

1. The APHSR method with the novel CSK index exhibited an excellent capability of bearing fault extraction. In the proposed method, a novel CSK was designed based on the advantages of the kurtosis function and cross-correlation function to quantitatively evaluate the detection ability of the bearing fault system under the background of complex noise in the frequency domain. The vibration signal was an incipient signal that was related to the fault feature.
2. The proposed method presented an outstanding capability to detect the bearing fault frequency of a wind power generator. It was easier to recognize the feature frequency of the bearing fault after the proposed method. The SNR value of the output outer ring and inner ring signals of the proposed CSK-based APHSR method increased by 3.9185 dB and 7.3528 dB when compared with the CSKMCCK-based USR method. The results demonstrated the outstanding performance of the CSK-based APHSR method to extract the fault features of bearings embedded in complex noise.
3. Further research was conducted with machine learning based on the medium tree method to reveal the superiority of the APHSR method based on CSK. The recognition rate of the bearing outer ring processed by the CSK-based APHSR method increased by 33% and 5% when compared with the original signals and the CSKMCCK-based USR method. The recognition rate of the bearing inner ring processed by the CSK-based APHSR method increased by 10% and 13% when compared with the original signals and the CSKMCCK-based USR method. The proposed method could more effectively enhance the performance of bearing fault feature extraction when the wind turbines worked in harsh environments.
4. As the computational cost is of great significant for the processing of bearing fault diagnosis, it will be studied as an important index to improve the ability of fault detection in the future.

Author Contributions: Conceptualization, S.W., Z.Q. and P.N.; methodology, S.W.; software, S.W.; validation, S.W.; formal analysis, S.W.; investigation, Z.Q.; resources, P.N.; data curation, P.N.; writing—original draft preparation, S.W.; writing—review and editing, S.W.; visualization, S.W.; supervision, Z.Q. and P.N.; project administration, Z.Q. and P.N.; funding acquisition, S.W., Z.Q. and P.N. All authors have read and agreed to the published version of the manuscript.

Funding: This research was funded by the Foundation of the State Key Laboratory of Performance Monitoring and Protection of Rail Transit Infrastructure of East China Jiaotong University (HJGZ2021114), National Natural Science Foundation of China (52205569), Zhejiang Provincial Natural Science Foundation of China (LQ22E050003), Shandong Provincial Innovation Ability Improvement Project of Middle and Small-sized High-tech Enterprises (2022TSGC2364), Ningbo Natural Science Foundation (2022J132), Laboratory of Yangjiang Offshore Wind Power (YJOFWD-OF-2022A08), Chuying Planning Project of Zhejiang Provincial Administration for Market Regulation (CY2023328), Ningbo Science and Technology Major Project (2020Z110, 2022Z057, 2022Z002), and the Application of Key Technologies of Intelligent Robot Process Automation (1500/2022-72002 B).

Data Availability Statement: Not applicable.

Acknowledgments: The authors are grateful to anonymous reviewers for their valuable comments and suggestions.

Conflicts of Interest: The authors declare no conflict of interest.

References

1. Alanazi, A.; Alanaz, M.; Nowdeh, S.A.; Abdelaziz, A.Y.; Siada, A. Stochastic-metaheuristic model for multi-criteria allocation of wind energy resources in distribution network using improved equilibrium optimization algorithm. *Electronics* **2022**, *11*, 3285. [CrossRef]
2. Torsvik, J.; Nejad, A.; Pedersen, E. Experimental field study of floater motion effects on a main bearing in a full-scale spar floating wind turbine. *Mar. Struct.* **2021**, *79*, 103059. [CrossRef]
3. Yoo, D.; Kang, S.; Jang, G.; Jung, S. Development of reactive power allocation method for radial structure wind farm considering multiple connections. *Electronics* **2022**, *11*, 2176. [CrossRef]
4. Xu, X.; Hu, S.; Shi, P.; Shao, H.; Li, R.; Li, Z. Natural phase space reconstruction-based broad learning system for short-term wind speed prediction: Case studies of an offshore wind farm. *Energy* **2023**, *262*, 125342. [CrossRef]
5. Esmaeili Shayan, M.; Najafi, G.; Ghobadian, B.; Gorjian, S.; Mamat, R.; Fairusham Ghazali, M. Multi-microgrid optimization and energy management under boost voltage converter with Markov prediction chain and dynamic decision algorithm. *Renew. Energy* **2022**, *201*, 179–189. [CrossRef]
6. Esmaeili Shayan, M.; Najafi, G.; Lorenzini, G. Phase change material mixed with chloride salt graphite foam infiltration for latent heat storage applications at higher temperatures and pressures. *Int. J. Energy Environ. Eng.* **2022**, *13*, 739–749. [CrossRef]
7. Loren, K.; Christopher, O. Health effects and wind turbines: A review of the literature. *Environ. Health* **2011**, *78*, 78.
8. Sa, J.W. Technical analysis of condition monitoring and fault diagnosis for wind turbines. *Water Resour. Electr. Pow. Constr.* **2021**, *7*, 177–178.
9. Xue, X.; Sang, S.; Huang, J. Flexible frequency response strategy with smooth rotor speed recovery of a DFIG-Based wind turbine. *Electronics* **2023**, *12*, 794. [CrossRef]
10. Johnson, K.; Fleming, P. Development, implementation, and testing of fault detection strategies on the national wind technology Center's controls advanced research turbines. *Mechatronics* **2010**, *21*, 728–736. [CrossRef]
11. Esmaeili Shayan, M.; Najafi, G.; Ghobadian, B.; Gorjian, S.; Mazlan, M.; Samami, M. Flexible Photovoltaic System on Non-Conventional Surfaces: A Techno-Economic Analysis. *Sustainability* **2022**, *14*, 3566. [CrossRef]
12. Cui, L.; Yang, J.; Wang, L.; Liu, H. Adaptive unsaturated bistable stochastic resonance multi-frequency signals detection based on preprocessing. *Electronics* **2021**, *10*, 2055. [CrossRef]
13. Benzi, R.; Sutera, A.; Vulpiani, A. The mechanism of stochastic resonance. *J. Phys. A* **1981**, *14*, L453–L457. [CrossRef]
14. Huang, W.; Zhang, G.; Jiao, S.; Wang, J. Bearing fault diagnosis based on stochastic resonance and improved whale optimization algorithm. *Electronics* **2022**, *11*, 2185. [CrossRef]
15. Herp, J.; Ramezani, M.H.; Andersen, M.; Niels, S.; Esmaeil, S. Bayesian state prediction of wind turbine bearing failure. *Renew. Energ.* **2018**, *116*, 164–172. [CrossRef]
16. Shi, P.; An, S.; Li, P.; Han, D. Signal feature extraction based on cascaded multi-stable stochastic resonance denoising and EMD method. *Measurement* **2016**, *90*, 318–328. [CrossRef]
17. Xu, Z.; Mei, X.; Wang, X.; Yue, M.; Jin, J.; Yang, Y.; Li, C. Fault diagnosis of wind turbine bearing using a multi-scale convolutional neural network with bidirectional long short term memory and weighted majority voting for multi-sensors. *Renew. Energy* **2022**, *183*, 615–626. [CrossRef]
18. Wang, S.; Niu, P.; Qiao, Z.; Guo, Y.; Wang, F.; Xu, C.; Han, S.; Wang, Y. Maximum cross-correlated kurtosis based unsaturated stochastic resonance and its application to bearing fault diagnosis. *Chin. J. Phys.* **2021**, *72*, 425–435. [CrossRef]
19. Lu, S.; He, Q.; Hu, F.; Kong, F. Sequential multiscale noise tuning stochastic resonance for train bearing fault diagnosis in an embedded system. *IEEE T. Instrum. Meas.* **2014**, *63*, 106–116. [CrossRef]
20. Li, J.; Li, M.; Zhang, J.; Jiang, G. Frequency-shift multiscale noise tuning stochastic resonance method for fault diagnosis of generator bearing in wind turbinehang. *Measurement* **2019**, *133*, 421–432. [CrossRef]
21. Yang, G.; Xia, J.; Kong, Y.; Tang, H. Weak fault feature extraction of rolling bearing based on reconstructed TFSR. *J. Mil. Transport. Acad.* **2020**, *22*, 90–95.
22. Li, Z.; Shi, B. A piecewise nonlinear stochastic resonance method and its application to incipient fault diagnosis of machinery. *Chin. J. Phys.* **2019**, *59*, 126–137. [CrossRef]
23. Antoni, J. Fast computation of the kurtogram for the detection of transient faults. *Mech. Syst. Signal Process.* **2007**, *21*, 108–124. [CrossRef]
24. Elforjani, M.; Shanbr, S.; Bechoefer, E. Detection of faulty high speed wind turbine bearing using signal intensity estimator technique. *Wind Energy* **2017**, *21*, 53–69. [CrossRef]
25. Jing, Z.; Guo, L. Hydraulic pump vibration signal pretreatment based on adaptive stochastic resonance with a general correlation function. *J. Vib. Shock* **2016**, *35*, 607–613.
26. Tao, Z.; Lu, C.; Zha, Z.; Lu, J.; Xiao, M. Multi-frequency periodic weak signal detection based on single-well potential stochastic resonance. *J. Electr. Meas. Instr.* **2014**, *28*, 72–85.
27. Wang, S.; Niu, P.; Guo, Y.; Wang, F.; Li, W.; Shi, H.; Han, S. Early diagnosis of bearing faults based on decomposition and reconstruction stochastic resonance system. *Measurement* **2018**, *158*, 107709. [CrossRef]
28. Lai, Z. *Weak-Signal Detection Based on the Chaotic and Stochastic-Resonance Characteristic of Duffing Oscillator*; Tianjin University: Tianjin, China, 2014.
29. Qin, G.; Gong, D.; Hu, G.; Wen, X. An analog simulation of stochastic resonance. *Acta Phys. Sin.* **1992**, *41*, 360–369.

30. Pascual, J.C.; Ordonez, J.G.; Morillo, M. Stochastic resonance: Theory and numerics. *Chaos* **2015**, *15*, 26115. [CrossRef]
31. Gammaitoni, L.; Hanggi, P.; Jung, P. Stochastic resonance. *Rev. Mod. Phys.* **1998**, *86*, 223–287. [CrossRef]
32. Qiao, Z.; Shu, X. Coupled neurons with multi-objective optimization benefit incipient fault identification of machinery. *Chaos Soliton. Fract.* **2021**, *145*, 110813. [CrossRef]
33. Antoni, J. The spectral kurtosis: A useful tool for characterizing non-stationary signals. *Mech. Syst. Signal Process.* **2006**, *20*, 282–307. [CrossRef]
34. Chen, X.; Zhang, B.; Feng, F.; Jiang, P. Optimal resonant band demodulation based on an improved correlated kurtosis and its application in bearing fault diagnosis. *Sensor* **2017**, *17*, 360. [CrossRef]
35. Lv, S. Research on rotor fault feature extraction method based on correlation coefficient principle EMD. *Mod. Manuf. Technol. Equipment.* **2018**, *6*, 54–55.
36. Antoni, J. The infogram: Entropic evidence of the signature of repetitive transients. *Mech. Syst. Signal Process.* **2016**, *74*, 73–94. [CrossRef]
37. Ho, D.; Randall, R.B. Optimisation of bearing diagnostic techniques using simulated and actual bearing fault signals. *Mech. Syst. Signal Process.* **2000**, *14*, 763–788. [CrossRef]
38. Mottershead, J.E.; Mares, C.; James, S.; Friswell, M.I. Stochastic model updating: Part 2-application to a set of physical structures. *Mech. Syst. Signal Process.* **2006**, *20*, 2171–2185. [CrossRef]
39. Wang, S.; Niu, P.; Guo, Y.; Wang, F.; Ma, X.; Han, L.; Wang, Y. Research on bearing fault diagnosis based on adaptive segmented hybrid system. *J. Aerod.* **2021**, *36*, 2090–2100.